Tropical Pacific Forcing of Decadal SST Variability in the Western Indian Ocean over the Past Two Centuries

Julia E. Cole,[1]* Robert B. Dunbar,[2] Timothy R. McClanahan,[3] Nyawira A. Muthiga[4]

A 194-year annual record of skeletal $\delta^{18}O$ from a coral growing at Malindi, Kenya, preserves a history of sea surface temperature (SST) change that is coherent with instrumental and proxy records of tropical Pacific climate variability over interannual to decadal periods. This variability is superimposed on a warming of as much as 1.3°C since the early 1800s. These results suggest that the tropical Pacific imparts substantial decadal climate variability to the western Indian Ocean and, by implication, may force decadal variability in other regions with strong El Niño–Southern Oscillation teleconnections.

In the Indian Ocean, SST variability reflects the influence of El Niño–Southern Oscillation (ENSO) and both forces and feeds back on the monsoons of India and East Africa (*1*). Over the past few decades, ENSO, the monsoons, and Indian Ocean SST appear to be associated, although the association is complex (*2–5*) and is likely to represent multiple feedbacks among these and other components of regional climate. Analysis of how these relations vary, particularly on decadal and longer time scales, is hampered by the limited instrumental SST record, which rarely spans more than the past few decades (*6*). Here, we present a 194-year proxy record of SST from Malindi Marine Park, Kenya, that allows us to examine the long-term relation between SST variability in the western Indian Ocean and variations in records of ENSO and other tropical climate phenomena, including a coral record from the Seychelles (*7*).

Climate variability in the western Indian Ocean–coastal East Africa region reflects the influence of seasonally changing SST, currents, and atmospheric convergence zones (*8*), combined with interannual and longer term variability that is often, but not always, associated with ENSO variability. Warm ENSO extremes generate warmer than usual SST off the Kenya coast, and these warm temperatures are associated with greater coastal rainfall during the shorter of the two rainy seasons (October–November) (*9, 10*). Recent Pacific climate trends, notably warmer temperatures since 1976 (*11*), also influence Indian Ocean SST fields (*5, 6*). However, the Indian Ocean also exhibits variability that appears unrelated to Pacific phenomena (*4, 5, 10*). The limited spatial and temporal scope of the instrumental record in the tropical Indian Ocean restricts the ability to study decadal and longer time scales of climate variability. This data gap can be addressed with high-fidelity paleoclimate records from long-lived corals. For example, a recent study used a 147-year coral record from the Seychelles to distinguish between interannual ENSO-related variability and decadal variability associated with the Asian monsoon (*7*).

Observed decadal climate variability is often difficult to attribute to specific forcings, because few climate forcings (except solar variability) act on strongly decadal time scales. However, recent work has identified decadal variability with ENSO-like features in the tropical Pacific (*12*). Because ENSO influences interannual climate variability in many parts of the world remote from the tropical Pacific (*3, 13*), one might expect such variability to propagate over a broad scale. However, decadal variability that originates from the tropical Pacific has not been clearly identified outside the Pacific Basin or before the 1976 shift. Because the 1976 shift may be related to anthropogenic greenhouse forcing of climate (*14*), analysis of this shift may not illuminate the natural modes of decadal variability in the Pacific or related regions.

We sampled core MAL-95-3, collected by hydraulic drill from a living colony of *Porites lutea* in Malindi Marine Park, Kenya (3°S, 40°E), in March 1995. The reef site lies at a depth of ~6 m (low tide), and the colony is ~4 m in height. The site is seasonally influenced by discharge from the Sabaki River, located 15 km north of the sampling site, but is otherwise well exposed to the open ocean, lying at the northern end of Kenya's fringing reef. X-radiographs of coral slabs show clear and regular density bands, and exposure of the cores to ultraviolet light revealed regular annual fluorescent bands (*15*). The fluorescent bands fall just above the top of the low-density band and are thought to reflect terrestrial input of fulvic acids from the Sabaki River (*16*), whose local influence peaks in December (*17*). Using density and fluorescent bands, we developed an annually precise age model; the core spans the interval 1801–1995 and exhibits an average growth rate of 12 mm/year. Monthly (1-mm resolution) isotopic and trace element records (*18*) show clear seasonality consistent with the low-density band forming between August and November, as SST warms seasonally from its August minimum.

We cut annual increments from the skeleton at the top of each clearly visible low-density band and crushed the sample to produce powder for isotopic analysis (Fig. 1) (*19*). Each increment represents 1 year, roughly November through October. This coarse sampling strategy may have smoothed the year-to-year variability—if, for example, the cut was not precisely along a time-stratigraphic boundary—but potential age offsets are likely less than 1 to 2 months.

The coral $\delta^{18}O$ record from this site reflects primarily SST; a linear regression of coral $\delta^{18}O$ versus SST yields a slope of −0.24 per mil (‰) $\delta^{18}O$ per 1°C, explaining 47% of the SST variance (*20*). Additional variability in coral $\delta^{18}O$ may arise from variations in the $\delta^{18}O$ of seawater due to precipitation, evaporation, or runoff, but at this site these changes are likely to be secondary because local rainfall $\delta^{18}O$ is not strongly depleted from average seawater (*21*) and salinity gradients are small (*22*). Rainfall and SST influences are likely to be additive in terms of annual effect on coral $\delta^{18}O$ because warmer years tend to be wetter at this site.

The 194-year coral $\delta^{18}O$ record indicates a trend toward lighter coral $\delta^{18}O$ that we interpret as primarily a temperature increase, although this trend may reflect contributions from both SST and salinity. If the record is interpreted strictly as temperature, then SST warmed by ~1.3° since 1801, and much of this warming occurred in the late 20th century. The coolest period since 1801 was the early 19th century, and the warmest SSTs followed a shift in 1976. A 1-year cooling of ~0.5°C followed several major volcanic eruptions, including Tambora (1815 erup-

[1]Department of Geological Sciences/Institute of Arctic and Alpine Research (INSTAAR)/Program in Atmospheric and Ocean Sciences, University of Colorado, Boulder, CO 80309, USA. [2]Department of Geological and Environmental Sciences, Stanford University, Stanford, CA 94305, USA. [3]The Wildlife Conservation Society, Coral Reef Conservation Project, Post Office Box 99470, Mombasa, Kenya. [4]Kenya Wildlife Service, Post Office Box 82144, Mombasa, Kenya.

*To whom correspondence should be addressed. Present address: Department of Geosciences, University of Arizona, Tucson, AZ 85721, USA.

tion), Krakatau (1883 eruption), and Agung (1963 eruption); this result is consistent with other data from the western Pacific (*23*).

The Malindi $\delta^{18}O$ time series also exhibits interannual and decadal variability. Using frequency domain analysis, we compared the Malindi $\delta^{18}O$ record and ENSO, represented by central Pacific SST anomalies (Niño 3.4) (*24*). Peaks in the variance spectra of the two records are coherent at a 5.5-year period (characteristic of ENSO) and in a broad decadal band (8 to 14 years). The presence of ENSO-related decadal variability is further indicated by the shift in 1976 to warmer and fresher conditions, a change seen in many tropical and north Pacific records (*25, 26*). At Malindi, this shift leads into the unusually warm conditions of the remainder of the coral record (1977–1994) and presumably sets the stage for the unprecedented warming and associated climate and environmental anomalies of 1997 (*10*), which precipitated large-scale coral bleaching and death (*27*).

To identify common trends and features related to broad-scale climate variability, we compared the Malindi $\delta^{18}O$ record with the 147-year coral $\delta^{18}O$ record from the Seychelles (5°S, 56°E) (*7*). The Malindi and Seychelles records agree substantially in time and frequency domains (Figs. 1 and 2B). For example, from the mid-1800s to the 1980s, both coral $\delta^{18}O$ records decrease by ~0.15‰, consistent with a warming of ~0.6°C; a comparable trend appears in the long-term Comprehensive Ocean-Atmosphere Data Set (COADS) SST data during the 20th century. The Malindi record shows additional warming of ~0.6°C in the interval 1800–1840, before the Seychelles or instrumental records begin.

Using a multitaper method with red noise assumptions to account for temporal persistence (*28*), we performed cross-spectral analysis between Malindi coral $\delta^{18}O$ and several other long Indo-Pacific records, including the Seychelles $\delta^{18}O$, Niño 3.4 SST, the All-India Rainfall Index (*29*), and an East African rainfall index (*30*). The Malindi record is coherent with the Seychelles and Niño 3.4 records at periods centered at 5.5 and 10 to 12 years (Fig. 2, A and B). The Seychelles record is also coherent with Niño 3.4 SST at these periods (*7*). Coherency between the Malindi record and regional rainfall indices (representing the monsoon) are weaker (Fig. 2, C and D). Figure 3 shows the filtered decadal 8- to 16-year component of all of these records. Over most of the common period, the coral and Niño 3.4 records are in phase and covary in amplitude (Fig. 3); the exception occurs during the 1930–1965 interval, when ENSO was relatively weak (*26, 31*). However, the rainfall indices, representing monsoon intensity in India and East Africa, show a weaker and more variable relation with each other and with all the other records.

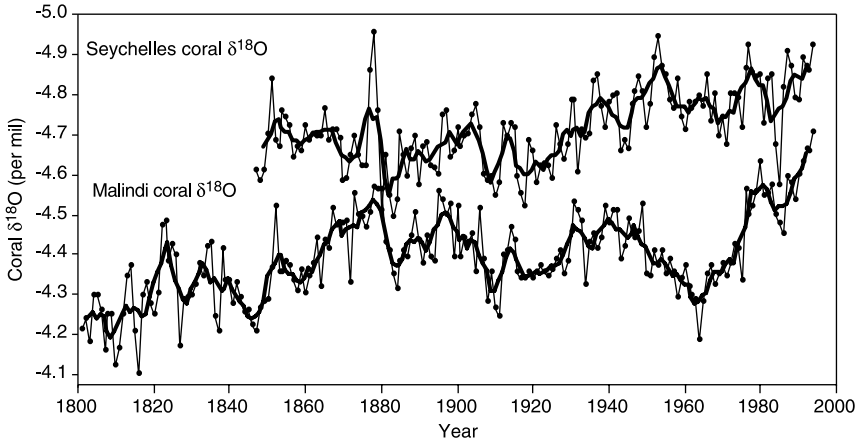

Fig. 1. Annual record of coral $\delta^{18}O$ from Malindi, Kenya, compared with annual record of coral $\delta^{18}O$ from Seychelles (*7*). Dark lines represent 5-year smoothing to highlight similar decadal variability in the corals. Seychelles data are presented as annual (November to October) to match the Malindi resolution and timing. Our calibration of temperature-$\delta^{18}O$ variability indicates that 1°C warming is represented by 0.24‰ decrease of $\delta^{18}O$.

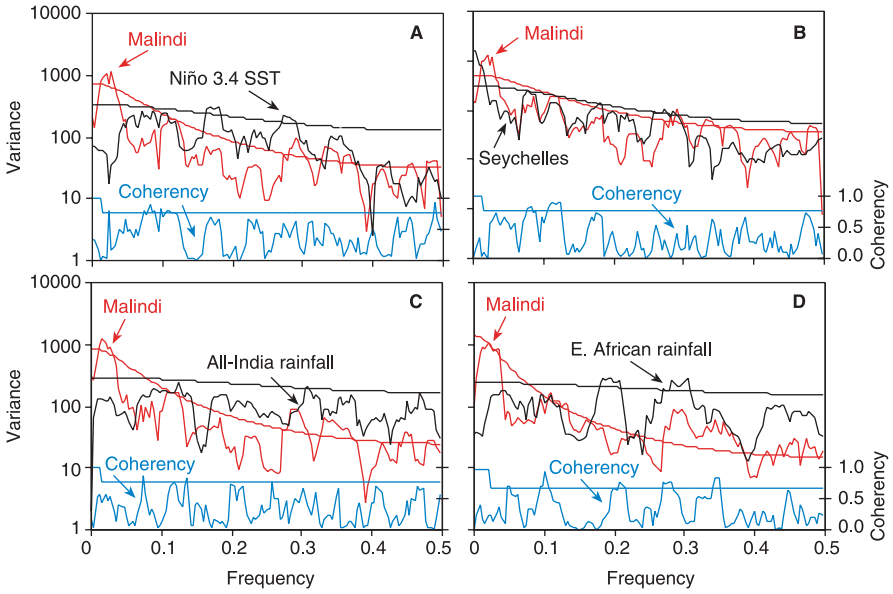

Fig. 2. Variance spectra and coherence of Malindi coral $\delta^{18}O$ and (**A**) Niño 3.4 SST (1856–1992), (**B**) Seychelles coral $\delta^{18}O$ (1847–1994), (**C**) All-India rainfall index (1871–1994), and (**D**) East African rainfall index (1892–1991). Malindi spectra differ slightly in each panel because slightly different time intervals were used, as noted. Coherence at decadal periods with the Malindi record is high for the Seychelles and Niño 3.4 records, but lower for the monsoon indices (India and east Africa rain).

The decadal component of the Malindi coral record reflects a regional climate signal spanning much of the western equatorial Indian Ocean. Previous work suggested a distinction between interannual ENSO and decadal monsoon influences (*7*). However, decadal variance in both the Malindi and Seychelles records is more coherent with ENSO indices than with the India or East Africa rain indices. The coherency of both coral records with Pacific indicators and with each other suggests instead that the Indian Ocean decadal variability reflects decadal ENSO-like variability originating in the Pacific. If the decadal variability in the coral records represents monsoon forcing, then the coherence between the coral and Niño 3.4 records requires a mechanism by which decadal variance in the monsoon generates or is greatly amplified by Pacific decadal variability.

Alternatively, the decadal variability in the Indian and Pacific oceans could represent a large-scale, consistent response to one or more other forcings. However, no obvious alternative global forcing (for example, solar variability) correlates with the decadal component of these records. We thus suggest that decadal variability in the coral records is primarily a response to Pacific influences, on

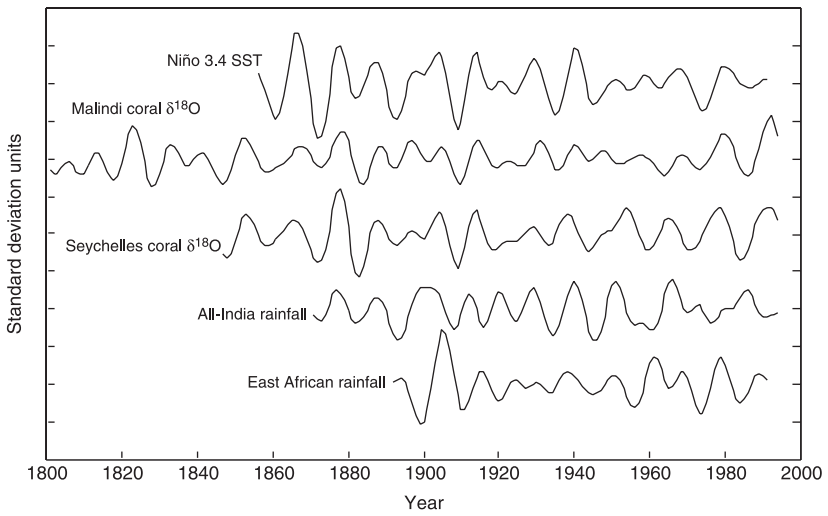

Fig. 3. Decadal components of the records used in Fig. 2, A to D, filtered from annual records with a Gaussian filter centered at a frequency of 0.0909 ± 0.03 years (center 11 years, range 8.3 to 16.4 years). All records are plotted so that the expected direction of influence of a warm ENSO phase is upward (the coral and India rainfall records are plotted inversely; the Niño 3.4 and East African rainfall records are oriented normally). The coral records and Niño 3.4 show similar patterns of variance; the rainfall records are more variable in their correlation with both the coral and the Niño 3.4 SST.

the basis of (i) the statistical hierarchy of stronger correlations with Niño 3.4 than with monsoon rain indices, and (ii) the well-documented capability of the tropical Pacific to amplify and propagate climate anomalies, particularly in the monsoon region (*3, 13*).

Our results do not address the issue of whether this decadal forcing originates from tropical or mid-latitude Pacific sources (*32*). However, a lack of decadal coherency between the Malindi record and the Pacific Decadal Oscillation (*33*) suggests that the tropical Pacific is more important in amplifying and propagating this signal, whatever its origin. Overall, these results suggest that the tropical Pacific is a strong candidate for the forcing of decadal climate variability wherever interannual ENSO anomalies produce consistent teleconnections.

References and Notes

1. S. Hastenrath, *Climate and Circulation of the Tropics* (Reidel, Dordrecht, Netherlands, 1988).
2. J. Shukla, in *Monsoons*, J. Fein and P. Stephens, Eds. (Wiley, New York, 1987), pp. 399–464; P. J. Webster and S. Yang, *Q. J. R. Meteorol. Soc.* **118**, 877 (1992); A. D. Vernekar, J. Zhou, J. Shukla, *J. Clim.* **8**, 248 (1995); G. A. Meehl, *Science* **266**, 263 (1994); *J. Clim.* **10**, 1921 (1997).
3. G. Kiladis and H. Diaz, *J. Clim.* **2**, 1069 (1989).
4. P. J. Webster *et al.*, *J. Geophys. Res.* **103**, 14451 (1998).
5. C. O. Clark, J. E. Cole, P. J. Webster, *J. Clim.*, in press.
6. P. Terray, *J. Clim.* **8**, 2595 (1995).
7. C. D. Charles, D. E. Hunter, R. G. Fairbanks, *Science* **277**, 925 (1997); data are available from the World Data Center–A for Paleoclimatology (www.ngdc.noaa.gov/paleo/paleo.html).
8. T. R. McClanahan, *Mar. Ecol. Prog. Ser.* **44**, 191 (1988).
9. S. E. Nicholson and D. Entekhabit, *Archiv. Meteor. Geophys. Bioclim.* **34**, 311 (1986); P. Hutchinson, *J. Clim.* **5**, 525 (1992); L. J. Ogallo, *J. Climatol.* **7**, 1 (1987); S. Hastenrath, A. Nicklis, L. Greischar, *J. Geophys. Res.* **98**, 20219 (1993).
10. P. J. Webster, J. Loschnigg, A. Moore, M. Reban, *Nature* **401**, 356 (1999).
11. N. E. Graham, T. P. Barnett, R. Wilde, M. Ponater, S. Schubert, *J. Clim.* **7**, 1416 (1994); K. E. Trenberth and J. W. Hurrell, *Clim. Dyn.* **9**, 303 (1994).
12. Y. Zhang, J. M. Wallace, D. S. Battisti, *J. Clim.* **10**, 1004 (1997).
13. C. F. Ropelewski and M. S. Halpert, *Mon. Weather Rev.* **115**, 1606 (1987); M. S. Halpert and C. F. Ropelewski, *J. Clim.* **5**, 577 (1992); K. E. Trenberth *et al.*, *J. Geophys. Res.* **103**, 14291 (1998).
14. N. E. Graham, *Science* **267**, 686 (1995).
15. Image of density and fluorescent bands in core MAL-96-1, from the same colony, can be seen at www.ogp.noaa.gov/misc/coral/coral_paleo/coraldata.html#Kenya.
16. P. J. Isdale, B. J. Stewart, J. M. Lough, *Holocene* **8**, 1 (1998).
17. T. R. McClanahan and D. Obura, *J. Exp. Mar. Biol. Ecol.* **209**, 103 (1995).
18. J. E. Cole, R. B. Dunbar, T. R. McClanahan, N. A. Muthiga, data not shown.
19. Stable isotope samples were analyzed on four isotope ratio mass spectrometers: a VG 602 with SIRA-series electronics at Rice University, a Finnigan 252 with Kiel device at Stanford University, a VG-SIRA with automated carbonate preparation device, and a Micromass Optima with automated carbonate preparation device, the latter two at the University of Colorado, Boulder (INSTAAR). The oxygen isotopic record represents duplicate (in some cases, triplicate) values for all samples. Each measurement has an analytical uncertainty of ±0.08‰.
20. We calibrate the coral $\delta^{18}O$ to the enhanced COADS SST from 3°S, 41°E, which has a broader screening tolerance than the standard COADS (4.5σ versus 3.5σ) to capture larger anomalies. COADS enhanced data are provided by the National Oceanic and Atmospheric Administration–Cooperative Institute for Research in Environmental Sciences Climate Diagnostics Center, Boulder, CO, from their web site (www.cdc.noaa.gov/). We use annual SST data representing a November–October year and include only years that contain at least three observations from every month; this procedure yields a slope of −0.238‰ per 1°C and explains 47% of the SST variance. The details of the calibration procedure have little effect on the paleotemperature slope: Using the standard SST product instead of the enhanced yields a slope of −0.228; omitting the minimum requirement of three observations per month yields a slope of 0.262 for the enhanced COADS and 0.252 for the standard. These correlations are all significant at >99.9%. More rigorous screening—for example, requiring a higher number of monthly observations—reduces the number of data points in the analysis (and hence reduces the statistical significance) but does not change slopes significantly. We obtained all slopes using linear regression and assuming SST as the independent variable. Given the SST screening applied, this assumption seems better justified than alternative methods that assume comparable error in both variables [for example, reduced major axis; J. C. Davis, *Statistics and Data Analysis in Geology* (Wiley, New York, 1986); G. T. Shen and R. B. Dunbar, *Geochim. Cosmochim. Acta* **59**, 2009 (1995)].
21. Rainfall $\delta^{18}O$ values from stations in Kenya, Tanzania, and Uganda are consistent at −2.8‰ [International Atomic Energy Agency–World Meteorological Organization Global Network for Isotopes in Precipitation (GNIP Database, Release 2, May 1998; www.iaea.org/programs/ri/gnip/gnipmain.htm)].
22. S. Levitus, R. Burgett, T. P. Boyer, *LEVITUS94: World Ocean Atlas 1994* (U.S. Department of Commerce, Washington, DC, 1994; http://ingrid.ldgo.columbia.edu/SOURCES/.LEVITUS94/).
23. M. K. Gagan and A. R. Chivas, *Geophys. Res. Lett.* **22**, 1069 (1995); T. J. Crowley, T. M. Quinn, F. W. Taylor, C. Henin, P. Joannot, *Paleoceanography* **12**, 633 (1997).
24. The Niño 3.4 SST record reflects SST anomalies in the central equatorial Pacific region bounded by 5°S to 5°N, 120° to 170°W [A. Kaplan *et al.*, *J. Geophys. Res.* **103**, 18567 (1998); http://ingrid.ldgo.columbia.edu/SOURCES/.KAPLAN/.Indices/].
25. K. E. Trenberth, *Bull. Am. Meteorol. Soc.* **71**, 988 (1990); C. C. Ebbesmeyer *et al.*, in *Proceedings of the 7th Annual Pacific Climate (PACLIM) Workshop, April 1990*, J. L. Betancourt and V. L. Sharp, Eds. (Interagency Ecological Studies Program Tech. Rep. 26, California Dept. of Water Resources, Sacramento, CA, 1991), pp. 120–141.
26. J. E. Cole, R. G. Fairbanks, G. T. Shen, *Science* **262**, 1790 (1993).
27. T. R. McClanahan, unpublished data; C. Wilkinson, *The 1997–1998 Mass Bleaching Event Around the World* (www.aims.gov.au/pages/research/coral-bleaching/1997-98-mbe/mbe-00.html).
28. M. E. Mann and J. Lees, *Clim. Change* **33**, 409 (1996).
29. B. Parthasarathy, K. Rupa Kumar, D. R. Kothawale, *Meteor. Mag.* **121**, 174 (1992); data available at http://grads.iges.org/india/allindia.html.
30. M. Hulme, *Int. J. Climatol.* **12**, 685 (1992); East African rainfall index can be accessed at http://cdiac.esd.ornl.gov/cdiac.
31. K. E. Trenberth and D. J. Shea, *Mon. Weather Rev.* **115**, 3078 (1987); W. P. Elliott and J. K. Angell, *J. Clim.* **1**, 729 (1988); C. Torrence and P. J. Webster, *J. Clim.* **12**, 2679 (1999).
32. M. Latif and T. P. Barnett, *Science* **266**, 634 (1994); R.-H. Zhang, L. M. Rothstein, A. J. Busalacchi, *Nature* **391**, 879 (1998).
33. N. J. Mantua, S. R. Hare, Y. Zhang, J. M. Wallace, R. C. Francis, *Bull. Am. Meteorol. Soc.* **78**, 1069 (1997); coherency analysis with Malindi record not shown.

34. We thank the Kenya Wildlife Service and the Kenya Marine and Fisheries Research Institute (particularly E. Okemwa and J. Mariara) for logistical and field support. Laboratory analysis was facilitated by D. Mucciarone, C. Urban, B. Vaughn, and D. White. Our interpretations benefited from ongoing discussions with C. Charles, C. Clark, M. Mann, and P. Webster. Supported by NSF Climate Dynamics and Earth System History program grants ATM 94-10298 and OCE-9614137 (J.E.C.) and ATM 94-09779, OCE-9632287, and OCE-9896157 (R.B.D.).

29 July 1999; accepted 3 December 1999